Electrical Power Quality and Utilisation, Journal Vol. XII, No. 2, 2006

Unified Power Quality Conditioner in a Grid Connected Photovoltaic System

Marcelo C. CAVALCANTI, Gustavo M.S. AZEVEDO, Bruno A. AMARAL, and Francisco A.S. NEVES

Federal University of Pernambuco, Brazile

Summary: **This paper presents a system that provides photovoltaic generation as well as the functions of a unified power quality conditioner. The system can be controlled for current harmonics and reactive power compensation simultaneously by using a converter operating as active shunt filter. The other converter is used as active series filter and it compensates voltage harmonics or voltage sags and swells. Using only an inverter in photovoltaic energy conversion process, the system presents increased efficiency when compared to the conventional systems. The synchronous reference frame method is used to control the three-phase converters. Simulation results demonstrate the good performance of the proposed configuration. Experimental results corresponding to the operation of the series filter as voltage sag compensator are presented.**

Key words:
control systems, converters, energy conversion, photovoltaic power systems, power quality, solar energy

1. INTRODUCTION

Photovoltaic (PV) energy has great potential to supply energy with minimum impact on the environment, since it is clean and pollution free [1]. A large number of solar cells connected in series and parallel set up the photovoltaic or solar arrays. One way of using photovoltaic energy is in a distributed energy system as a peaking power source [2].

On the other hand, strict regulations have been applied to the equipment connected to the utility lines. Some of these regulations are related to harmonics distortion and power factor. However, with the development of power electronics, much equipment tends to increase the levels of harmonic distortion. The line current at the input to the diode bridge rectifier deviates significantly from a sinusoidal waveform and this distorted current can also lead to distortion in the line voltage. Moreover, much modern equipment uses digital controllers, based on microprocessors sensitive to variations in the voltage and current waveforms. Therefore, to increase the PV system utilization the power conversion can be designed to also provide functions of a unified power quality conditioner.

The utilization of two dc/ac fully controlled converters makes the system have the most versatile structure of converters applied as energy conditioner. In this case, depending on the controller, the converters can have different functions of compensation. For instance, they can realize active series and shunt filters combined to compensate simultaneously load current and harmonics of the supplied voltage [3]. In this way, the equipment is called Unified Power Quality Conditioner (UPQC) [4].

An active shunt filter is a suitable device for current-based compensation [5]. This configuration includes current harmonics and reactive power compensations. The active shunt filter can also balance unbalancing currents.

The active series filter is normally used for voltage-based compensation [5]. In this case, voltage harmonics and voltage sags and dips are compensated.

Other applications can be found in literature for purposes of compensation of the fundamental frequency, such as reactive power compensation, flux control of active power and voltage regulation. In this case, it is called Unified Power Flow Controller (UPFC) [6]-[7].

Conventionally, grid connected photovoltaic energy conversion systems are composed of a dc-dc converter and an inverter [1]-[2]. The dc-dc converter is controlled to track the maximum power point of the photovoltaic array and the inverter is controlled to produce current in such a way that the system current has low total harmonic distortion (THD) and it is in phase with the utility voltage. The efficiency of the conventional system is low because the dc-dc converter and the inverter are connected in series. The purpose of this paper is to design a photovoltaic generation system for connection in a three-phase system using only a dc/ac inverter. The proposed system increases the conversion efficiency and also provides useful function any time, operating as power supply as well as harmonic and reactive power compensator when the sun is available. At low irradiation, the system operates only as harmonic and reactive power compensator. Other dc/ac converter is used to provide voltage harmonic compensation. Cost estimation shows that the use of additional components increases the cost in less than 12% to have another function to improve power quality. Also this converter does not change the efficiency of the PV energy conversion since the converters are connected in parallel. The control was implemented with the synchronous reference frame (SRF) method. The system and controller were design and simulated. Different pulse-width-modulation (PWM) techniques have been compared to suggest a configuration with optimal efficiency. The system provides approximately 2.8 kW of photovoltaic generation.

2. GRID CONNECTED PHOTOVOLTAIC SYSTEM

The proposed photovoltaic (PV) energy conversion system has high efficiency, low cost and high functionality. Figure 1 shows the block diagram of the proposed system. The converter 1 (PV converter) in Figure 1 is responsible to convert the PV energy to the grid as well as to compensate

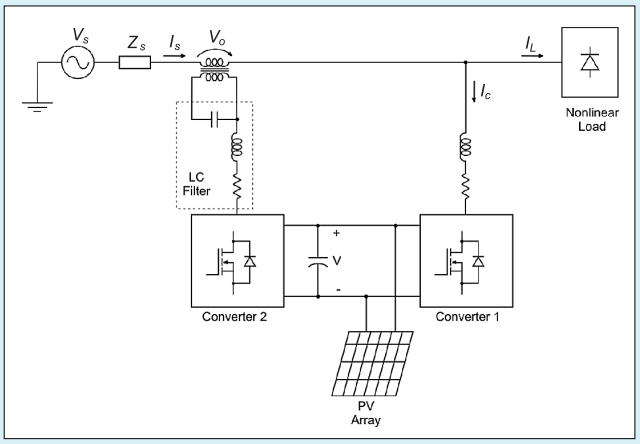

Fig. 1. Proposed system: PV generation with UPQC function

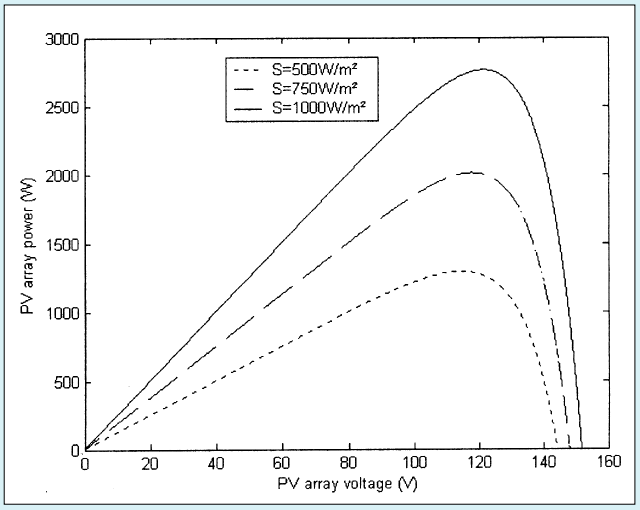

Fig. 2. Characteristic diagram of the solar array

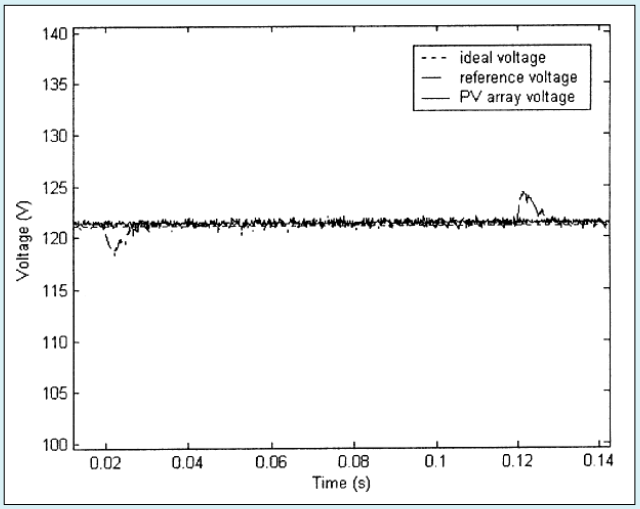

Fig. 3. MPPT controller: solar array output voltage

current harmonics and reactive power. The converter 2 (Dynamic Voltage Restorer – DVR converter) in Figure 1 is responsible to compensate voltage harmonics or voltage sags. The utilization of two controlled converters makes the system to have the most versatile structure applied as energy conditioner. In this case, depending on the controller, the converters can have different functions of compensation. For instance, they can realize active series and shunt filters combined to compensate simultaneously load current and harmonics of the supplied voltage.

3. MAXIMUM POWER POINT TRACKING

The controller of converter 1 in Figure 1 has to track the maximum power point of the photovoltaic array as well as to compensate harmonic and reactive power. When the system is operating as photovoltaic energy generator, the maximum power point tracking (MPPT) controller is used to calculate the reference voltage. When the system is operating only as harmonic and reactive power compensator, the reference voltage is constant [1].

It is important to operate the photovoltaic system near the maximum power point to increase the efficiency of photovoltaic arrays. A MPPT method often used is the perturbation and observation method [9]. However, in this paper, it is used the slope of power versus voltage, which decreases the oscillation problem and it is easy to implement [1]. The output power of the PV array and the differential of the output power to the output voltage can be expressed as:

$$P = V \cdot I \tag{1}$$

$$\frac{dP}{dV} \cong I + \frac{\Delta I}{\Delta V} \cdot V \tag{2}$$

where:
P — PV array output power.
V — PV array output voltage.
I — PV array output current.
ΔI — Increment of the PV array output current.
ΔV — Increment of the PV array output current.

In the method, (2) is used as the index of the maximum power point tracking operation (Fig. 2), where S is the solar irradiation. When $dP/dV<0$, decreasing the reference voltage forces dP/dV to approach zero; when $dP/dV>0$, increasing the reference voltage forces dP/dV to approach zero; when $dP/dV=0$, reference voltage does not need any change [1].

A voltage sag is simulated between 0.02 and 0.12s and the reference voltage generated by the MPPT algorithm has small oscillation around the ideal voltage at the beginning and the end of the short circuit (Fig. 3). The PV array voltage stays near to the ideal voltage that is around 121V. Even during the voltage sag, the MPPT algorithm presents very good results with at least 99% of the PV maximum output power.

4. CURRENT BASED COMPENSATION

Figure 4 shows the converter 1 connected to the grid. The converter is responsible to convert the PV energy to the grid as well as to compensate current harmonics and reactive power. Under balanced operating conditions, it is possible to express the inverter phase output voltages in terms of the inverter output voltages with respect to the negative dc bus:

$$v_{kn} = v_{kN} - v_{nN} \quad k = a,b,c \tag{3}$$

Each phase voltage can be written as:

$$v_{kn} = v_{Sk} - L_c \frac{di_{Ck}}{dt} \tag{4}$$

In a three-phase, three wire load:

$$v_{nN} = \frac{1}{3}\left(v_{aN} + v_{bN} + v_{cN}\right) \tag{5}$$

Substituting v_{nN} from (5) into (3):

$$v_{1n} = \frac{2}{3}v_{aN} - \frac{1}{3}v_{bN} - \frac{1}{3}v_{cN} \tag{6}$$

Similar equations can be written for phase *b* and *c* voltages. The phase voltages can be also written as:

$$\begin{bmatrix} v_{an} \\ v_{bn} \\ v_{cn} \end{bmatrix} = V \cdot \begin{bmatrix} 2/3 & -1/3 & -1/3 \\ -1/3 & 2/3 & -1/3 \\ -1/3 & -1/3 & 2/3 \end{bmatrix} \cdot \begin{bmatrix} T_1 \\ T_2 \\ T_3 \end{bmatrix} \tag{7}$$

where the variables T_k represent the states of the inverter upper switches. T_k is 0 for opened switches and 1 for closed switches. Defining d_k as swithing state function [8]:

$$\begin{bmatrix} d_a \\ d_b \\ d_c \end{bmatrix} = \frac{1}{3} \cdot \begin{bmatrix} 2 & -1 & -1 \\ -1 & 2 & -1 \\ -1 & -1 & 2 \end{bmatrix} \begin{bmatrix} T_a \\ T_b \\ T_c \end{bmatrix} \tag{8}$$

On the *dc* side:

$$\frac{dV}{dt} = \frac{i_{dc}}{C} = \frac{1}{C}\left(T_a \cdot i_{Ca} + T_b \cdot i_{Cb} + T_c \cdot i_{Cc}\right) \tag{9}$$

The complete model of the system (Fig. 4) in the *abc* referential is shown in (10) [8]:

$$\frac{d}{dt}\begin{bmatrix} i_{Ca} \\ i_{Cb} \\ V \end{bmatrix} = \begin{bmatrix} 0 & 0 & -\frac{d_a}{L_C} \\ 0 & 0 & -\frac{d_b}{L_C} \\ \frac{2d_a + d_b}{C} & \frac{d_a + 2d_b}{C} & 0 \end{bmatrix} \cdot \begin{bmatrix} i_{Ca} \\ i_{Cb} \\ V \end{bmatrix} + \frac{1}{L_C}\begin{bmatrix} v_{S1} \\ v_{S2} \\ 0 \end{bmatrix} \tag{10}$$

where:

i_{Ca}, i_{Cb}, i_{Cc} — three-phase converter 1 currents,
L_C — inductance of the transformer,
d_a, d_b, d_c — three-phase switching state functions,
C — capacitance of the dc link,
v_{Sa}, v_{Sb}, v_{Sc} — three-phase supply voltages.

In (10), the steady state fundamental components are sinusoidal. To reduce control complexity, the *dq* frame in (11) rotating at the supply frequency can be used. With this frame, the positive-sequence components at fundamental frequency become constant [8]:

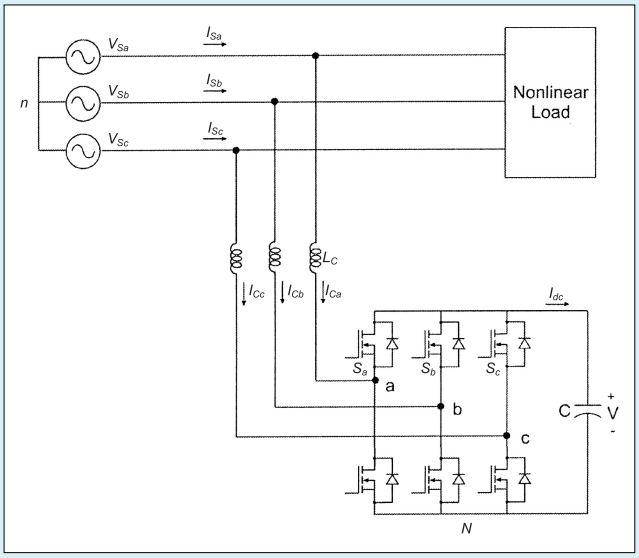

Fig. 4. Converter 1 connected to the grid

$$\begin{bmatrix} i_{Cd} \\ i_{Cq} \\ i_{C0} \end{bmatrix} = \tag{11}$$

$$= \sqrt{\frac{2}{3}} \begin{bmatrix} \cos\omega t & \cos\left(\omega t - 2\pi/3\right) & \cos\left(\omega t + 2\pi/3\right) \\ -\sin\omega t & -\sin\left(\omega t - 2\pi/3\right) & -\sin\left(\omega t + 2\pi/3\right) \\ 1/\sqrt{2} & 1/\sqrt{2} & 1/\sqrt{2} \end{bmatrix} \cdot \begin{bmatrix} i_{Ca} \\ i_{Cb} \\ i_{Cc} \end{bmatrix}$$

where:

i_{Cd}, i_{Cq} — D-axis and *q*-axis converter currents,
i_{C0} — zero-sequence converter current,
ω — supply angular frequency.

Taking into account the absence of the zero-sequence components in the currents in a three-wire system, the simplified transformation matrix can be used:

$$\begin{bmatrix} i_{Cd} \\ i_{Cq} \end{bmatrix} = \sqrt{2} \begin{bmatrix} \cos\left(\omega t - \pi/6\right) & \sin\omega t \\ -\sin\left(\omega t - \pi/6\right) & \cos\omega t \end{bmatrix} \cdot \begin{bmatrix} i_{Ca} \\ i_{Cb} \end{bmatrix} \tag{12}$$

The model in the *dq* frame is as in (13) [8]:

$$\frac{d}{dt}\begin{bmatrix} i_{Cd} \\ i_{Cq} \\ V \end{bmatrix} = \begin{bmatrix} 0 & \omega & -\frac{d_d}{L_C} \\ -\omega & 0 & -\frac{d_q}{L_C} \\ \frac{d_d}{C} & \frac{d_q}{C} & 0 \end{bmatrix} \cdot \begin{bmatrix} i_{Cd} \\ i_{Cq} \\ V \end{bmatrix} + \frac{1}{L_C}\begin{bmatrix} v_{Sd} \\ v_{Sq} \\ 0 \end{bmatrix} \tag{13}$$

where:

d_d, d_q — D-axis and q-axis switching state functions,
v_{Sd}, v_{Sq} — D-axis and q-axis supply voltages.

The current equations in the model (13) can be written as:

$$L_C \frac{di_{Cd}}{dt} = L_c \cdot \omega \cdot i_{Cq} - V \cdot d_d + v_{Sd} \tag{14}$$

$$L_C \frac{di_{Cq}}{dt} = -L_c \cdot \omega \cdot i_{Cd} - V \cdot d_q + v_{Sq} \tag{15}$$

Defining:

$$u_d = L_c \cdot \omega \cdot i_{Cq} - V \cdot d_d + v_{Sd} \tag{16}$$

$$u_q = -L_c \cdot \omega \cdot i_{Cd} - V \cdot d_q + v_{Sq} \tag{17}$$

and considering that the current control is realized by using PI compensators, the equations (18) and (19) in Figure 5 are:

$$d_d = \frac{v_{Sd} + L_C \cdot \omega \cdot i_{Cq} - u_d}{V} \tag{18}$$

$$d_q = \frac{v_{Sq} - L_C \cdot \omega \cdot i_{Cd} - u_q}{V} \tag{19}$$

where:

u_d — D-axis output of the current PI compensator.

u_q — Q-axis output of the current PI compensator.

The voltage equation in the model (13) can be written as:

$$C \frac{dV}{dt} = d_d \cdot i_{Cd} + d_q \cdot i_{Cq} \tag{20}$$

Defining:

$$u_{pv} = d_d \cdot i_{Cd} + d_q \cdot i_{Cq} \tag{21}$$

and considering that the voltage control is realized by using a PI compensator, the equation (22) in Figure 5 is:

$$i_{dcr} = \sqrt{\frac{2}{3}} \frac{V}{V_{sup}} u_{pv} \tag{22}$$

where:

u_{pv} — output of the voltage PI compensator,

V_{sup} — amplitude of the supply voltage.

Figure 5 shows the controller block diagram of converter 1 in Figure 1. The phase-locked-loop (PLL) circuit detects the amplitude and the position of the supply voltage vector. When the system is operating as photovoltaic energy generator, the MPPT controller is used to calculate the

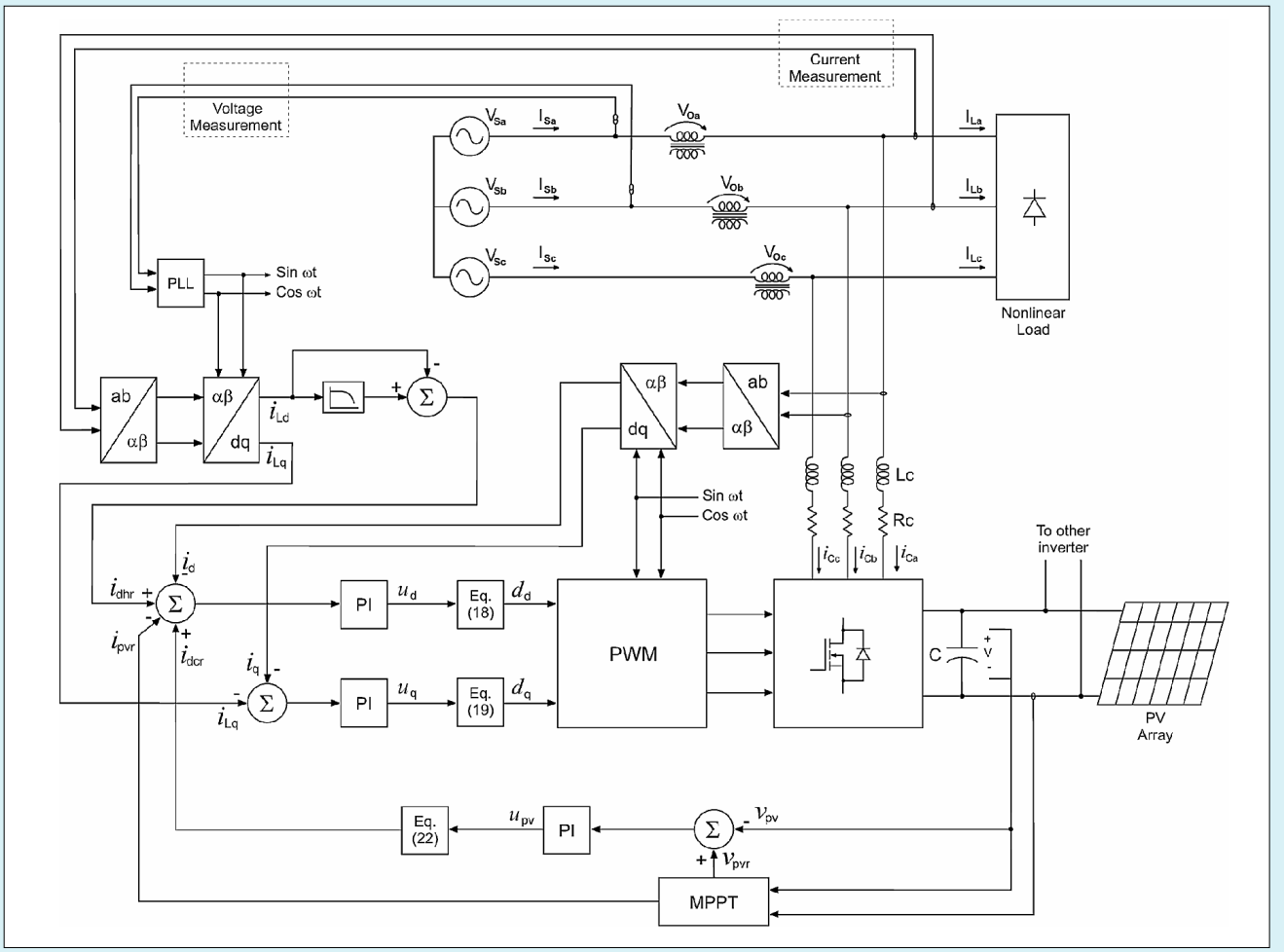

Fig. 5. Control of the proposed system: PV generation / current harmonic and reactive power compensations

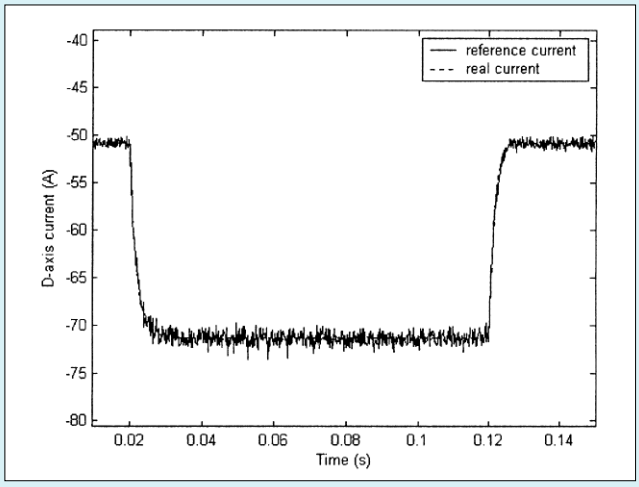

Fig. 6. Tracking performance of the *d*-axis current loop

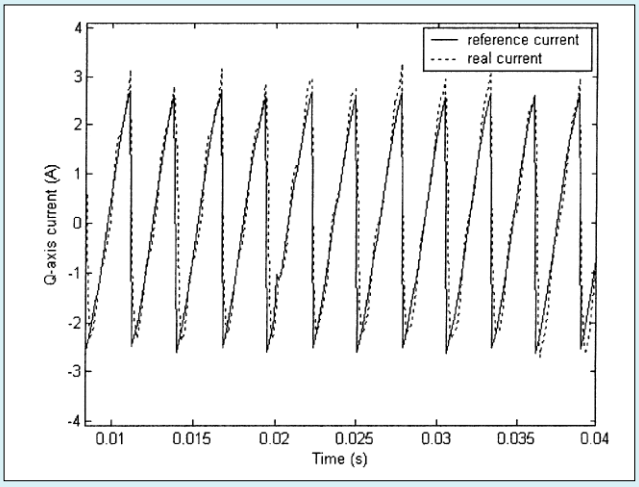

Fig. 7. Tracking performance of the *q*-axis current loop

reference voltage. When the system is operating only as current harmonic and reactive power compensator, the reference voltage is constant [1]. In the SRF, the fundamental positive-sequence components of the load appear as dc quantities [8]. Since the grid currents must have a sinusoidal waveform and be in phase with the grid voltage in the proposed design, the grid current has only *d*-axis component. Therefore, the *q*-axis reference current for the inverter is the q-axis load current [2]. The *d*-axis reference current is composed of three parts: reference d-axis load current (I_{dhr}), reference dc link current (I_{dcr}) and reference photovoltaic array current (I_{pvr}).

The *d*-axis load current is passed through a low pass filter that removes the high frequency components in the *d–q* reference frame. A first order low pass filter with a cut frequency of 20Hz is used. Subtracting the *d*-axis load current of the filtered *d*-axis load current, the result is the negative of the *d*-axis harmonics. This value is used as the reference *d*-axis load current since the positive current flows into the inverter. The *dc* component in the *d–q* reference frame corresponds to the fundamental component of the real power flowing to the load. The inverter dc link voltage controller calculates the current to maintain the *dc* link voltage by passing the *dc* link voltage error through a PI compensator. The current obtained by the MPPT controller corresponds to the real power available from the photovoltaic array and it is subtracted from the current components to maintain the dc link voltage and to compensate harmonics.

Using *d–q* reference frame, the coupled dynamics of the current tracking problem have been transformed into decoupled dynamics. By adjusting PI compensators, a fast tracking and zero steady state errors can be achieved. The results (Fig. 6 and Fig. 7) show that the oscillating current harmonics injected by the inverter track their references with high accuracy even during the voltage sag. The dc link current increases to keep the maximum power in PV array.

The controller can compensate harmonic and reactive power effectively as shown in Figure 8. Figure 8 shows that the supply current is displaced by 180 degrees because it is generated more power from the PV array than that needed for the load. Therefore, in this case the PV array supplies the load and injects power for the grid. In Figure 9, the load

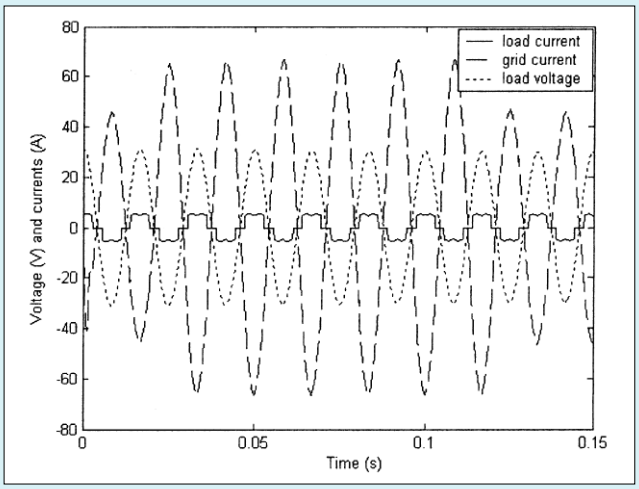

Fig. 8. Current harmonics and reactive power compensations

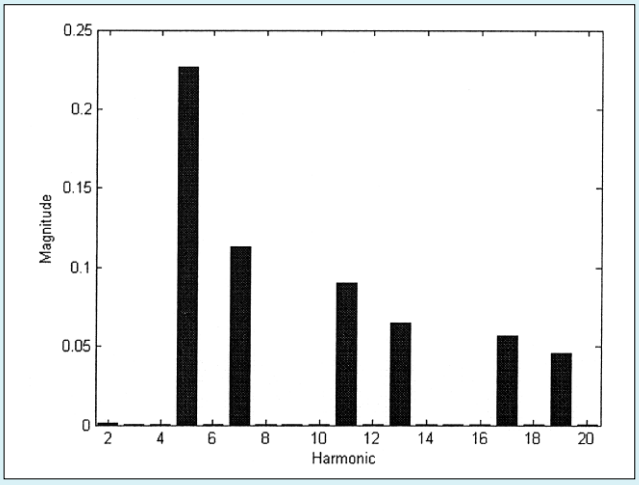

Fig. 9. Current harmonics for the load

fundamental current is used as magnitude 1 and it is not shown to allow that the harmonics can be analyzed. In Figure 10, the supply fundamental current is used as magnitude 1.

5. VOLTAGE BASED COMPENSATION

Figure 11 shows the converter 2 in Figure 1 connected to the grid. The voltage compensator is a system based on power electronics that detects the feeder voltage and in case

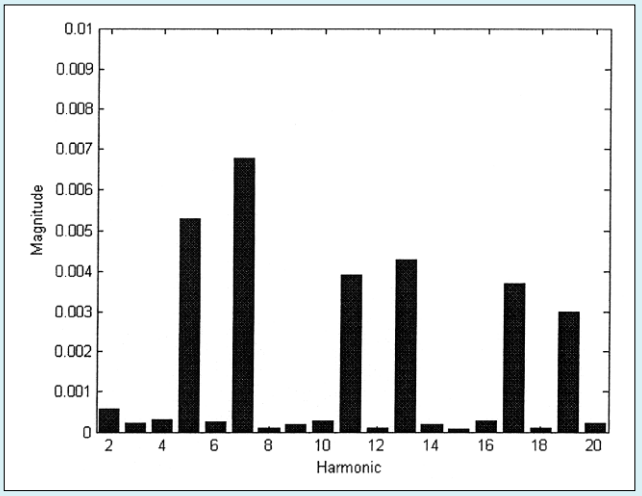

Fig. 10. Current harmonics for the supply

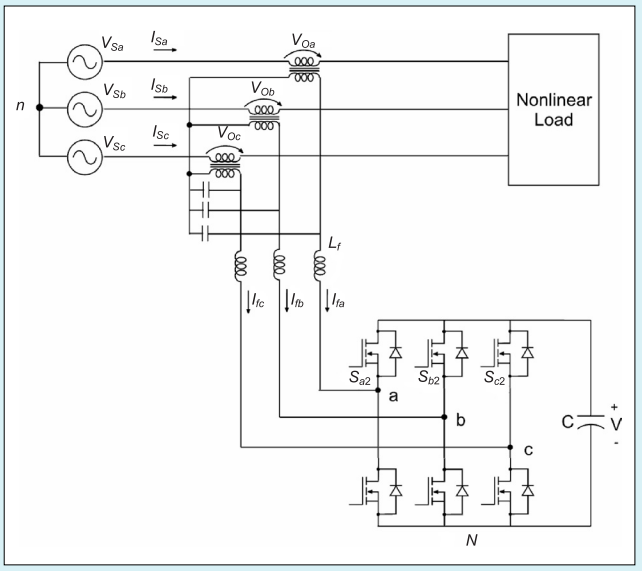

Fig. 11. Converter 2 connected to the grid

the voltage is different of the desired voltage, it supplies the necessary voltage to compensate the voltage error. It can be used to compensate voltage harmonics at the point of common coupling or voltage sags, keeping the load voltage around its rated value.

In this paper, it is presented the voltage sag compensation control. Its use is more justified when many sensitive loads are connected to the same feeder [10].

Under balanced operating conditions, it is possible to express the inverter phase output voltages in terms of the inverter output voltages with respect to the negative dc bus:

$$v_{k0} = v_{kN2} - v_{0N2} \qquad k = a,b,c \qquad (23)$$

Each phase voltage can be written as:

$$v_{k0} = v_{K0} - L_f \frac{di_{fk}}{dt} \qquad (24)$$

In a three-phase, three wire load:

$$v_{0N2} = \frac{1}{3}\left(v_{aN2} + v_{bN2} + v_{cN2}\right) \qquad (25)$$

The variables T_{k2} represent the states of the converter 2 upper switches. T_{k2} is 0 for opened switches and 1 for closed switches. Defining d_{k2} as swithing state function:

$$\begin{bmatrix} d_{a2} \\ d_{b2} \\ d_{c2} \end{bmatrix} = \frac{1}{3} \cdot \begin{bmatrix} 2 & -1 & -1 \\ -1 & 2 & -1 \\ -1 & -1 & 2 \end{bmatrix} \begin{bmatrix} T_{a2} \\ T_{b2} \\ T_{c2} \end{bmatrix} \qquad (26)$$

In the filter output voltage:

$$\frac{dv_{K0}}{dt} = -\frac{1}{C_f}\left(i_{fk} - i_{Lk}\right) \qquad (27)$$

The complete model of the system (Fig. 11) in the *abc* referential is shown in (28):

$$\frac{d}{dt}\begin{bmatrix} i_{fa} \\ i_{fb} \\ v_{0a} \\ v_{0b} \end{bmatrix} = \begin{bmatrix} 0 & 0 & \frac{1}{L_f} & 0 \\ 0 & 0 & 0 & \frac{1}{L_f} \\ -\frac{1}{C_f} & 0 & 0 & 0 \\ 0 & -\frac{1}{C_f} & 0 & 0 \end{bmatrix} \cdot \begin{bmatrix} i_{fa} \\ i_{fb} \\ v_{0a} \\ v_{0b} \end{bmatrix} + \begin{bmatrix} -\frac{d_{a2}}{L_f}V \\ -\frac{d_{b2}}{L_f}V \\ \frac{1}{C_f}i_{La} \\ \frac{1}{C_f}i_{Lb} \end{bmatrix} \qquad (28)$$

where:
i_{fa}, i_{fb}, i_{fc} — three-phase converter 2 currents,
L_f — inductance of the filter,
d_{a2}, d_{b2}, d_{c2} — three-phase switching state functions,
C_f — capacitance of the filter,
v_{0a}, v_{0b}, v_{0c} — three-phase filter output voltages.

In (28), the steady state fundamental components are sinusoidal. To reduce control complexity, the *dq* frame rotating at the supply frequency can be used. Taking into account the absence of the zero-sequence components in a three-wire system, the model in the *dq* frame is as in (29):

$$\frac{d}{dt}\begin{bmatrix} i_{fd} \\ i_{fq} \\ v_{0d} \\ v_{0q} \end{bmatrix} = \begin{bmatrix} 0 & \omega & \frac{1}{L_f} & 0 \\ -\omega & 0 & 0 & \frac{1}{L_f} \\ -\frac{1}{C_f} & 0 & 0 & \omega \\ 0 & -\frac{1}{C_f} & -\omega & 0 \end{bmatrix} \cdot \begin{bmatrix} i_{fd} \\ i_{fq} \\ v_{0d} \\ v_{0q} \end{bmatrix} + \begin{bmatrix} -\frac{d_{d2}}{L_f}V \\ -\frac{d_{q2}}{L_f}V \\ \frac{1}{C_f}i_{Ld} \\ \frac{1}{C_f}i_{Lq} \end{bmatrix} \qquad (29)$$

where:
d_{d2}, d_{q2} — D-axis and *q*-axis switching state functions.
v_{0d}, v_{0q} — D-axis and *q*-axis filter output voltages.

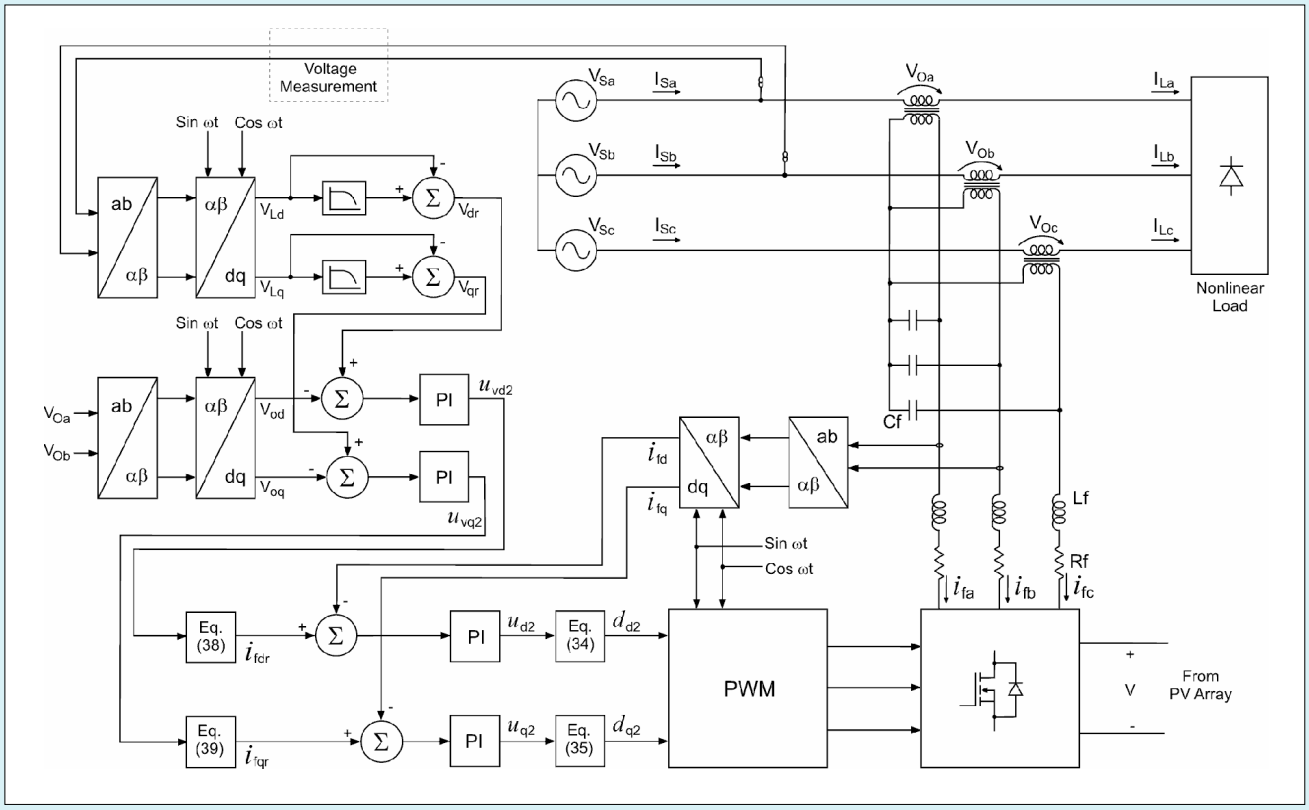

Fig. 12. Control of the proposed system: PV generation / current harmonic and reactive power compensations

The current equations in the model (29) can be written as:

$$L_f \frac{di_{fd}}{dt} = L_f \cdot \omega \cdot i_{fq} + v_{0d} - V \cdot d_{d2} \tag{30}$$

$$L_f \frac{di_{fq}}{dt} = -L_f \cdot \omega \cdot i_{fd} + v_{0q} - V \cdot d_{q2} \tag{31}$$

Defining:

$$u_{d2} = L_f \cdot \omega \cdot i_{fq} + v_{0d} - V \cdot d_{d2} \tag{32}$$

$$u_{q2} = -L_f \cdot \omega \cdot i_{fd} + v_{0q} - V \cdot d_{q2} \tag{33}$$

and considering that the current control is realized by using PI compensators, the equations (34) and (35) in Figure 12 are:

$$d_{d2} = \frac{v_{0d} + L_f \cdot \omega \cdot i_{fq} - u_{d2}}{V} \tag{34}$$

$$d_{q2} = \frac{v_{0q} - L_f \cdot \omega \cdot i_{fd} - u_{q2}}{V} \tag{35}$$

where:

u_{d2} — D-axis output of the current PI compensator,

u_{q2} — Q-axis output of the current PI compensator.

The voltage equations in the model (29) can be written as:

$$C_f \frac{dv_{0d}}{dt} = -i_{fd} + C_f \cdot \omega \cdot v_{0q} + i_{Ld} \tag{36}$$

$$C_f \frac{dv_{0q}}{dt} = -i_{fq} - C_f \cdot \omega \cdot v_{0d} + i_{Lq} \tag{37}$$

Therefore:

$$i_{fdr} = i_{Ld} + C_f \cdot \omega \cdot v_{0q} - u_{vd2} \tag{38}$$

$$i_{fqr} = i_{Lq} - C_f \cdot \omega \cdot v_{0d} - u_{vq2} \tag{39}$$

where:

u_{vd2} — D-axis output of the voltage PI compensator,

u_{vq2} — Q-axis output of the voltage PI compensator.

The voltage sag compensator (DVR) is composed basically of an energy storage system, a *dc*-link, a *dc–ac* converter and a transformer (Fig. 11).

To find out which voltage reference value should be in the load when voltage sag occurs, it is needed to determine the voltage value before the sag. The output signals of the PLL are used to inform in a very short time the values of V_d, V_q and θ. During the voltage sags, the variations in the angle θ originate another synchronous referential rotated in relation to the original reference angle θ* (Fig. 13).

One of the methods for generation of reference voltage is

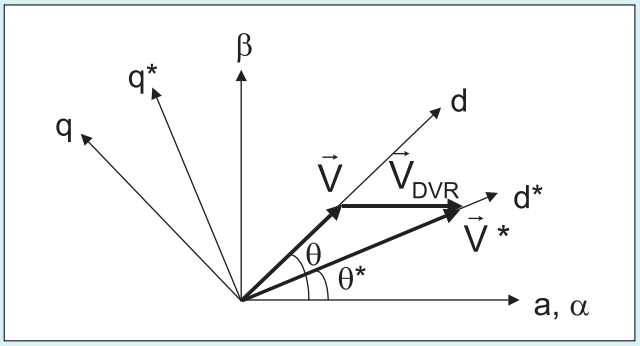

Fig 13. Reference axes system during a voltage sag

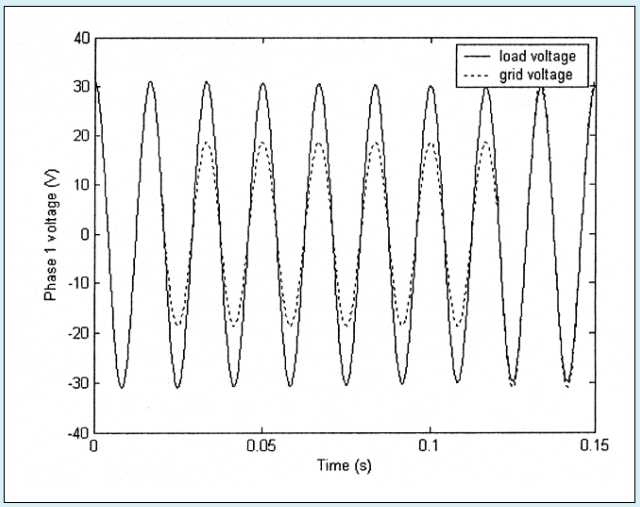

Fig. 14. Phase *a* voltages during the simulation

by using a low pass filter in the output signals of the PLL. This filter has a slow dynamic, in such a way that the difference between the reference signal and the grid signal is the voltage value that should be injected by the DVR to compensate the sag:

$$\Delta V_d = V_d^* - V_d \qquad (40)$$
$$\Delta V_q = V_q^* - V_q$$

From Figure 13:

$$V_{DVR,d} = V_d^* - V_S \cos\left(\theta - \theta^*\right)$$
$$V_{DVR,q} = V_q^* - V_S \quad \sin\left(\theta - \theta^*\right) \qquad (41)$$

Knowing that V_q* should be zero, (40) is simplified for:

$$V_{DVR,d} = V_d^* - V_S \cos\left(\theta - \theta^*\right)$$
$$V_{DVR,q} = -V_S \quad \sin\left(\theta - \theta^*\right) \qquad (42)$$

where:

V_d^* — D-axis load reference voltage,
V_q^* — Q-axis load reference voltage,
V_d — D-axis grid voltage,
V_q — Q-axis grid voltage,
$V_{DVR,d}$ — D-axis DVR reference voltage,
$V_{DVR,q}$ — Q-axis DVR reference voltage,
V_S — supply voltage vector,
θ — supply voltage vector angle,
θ^* — load reference voltage vector angle.

To determine which the value of reference angle θ*, instead of filtering the angle θ that is supplied by the PLL, it should be filtered the value of ω*. The output of this filter passes by an integer, supplying the reference angle.

The controller can compensate voltage sags effectively as shown in Figure 14. Figure 14 shows the phase 1 voltage for the supply and the load. Phases 2 and 3 also present effective compensation, keeping the rated voltage in the load.

The prototype of the DVR is composed of a capacitor set (*dc* link), an inverter, an output filter and a series transformer. It is also included a three-phase resistive load. The experimental tests have been realized with 380V (line-to-line voltage). The control system consists of a microcomputer with interfaces dedicated to measure the electrical variables and to command the converters switches.

To verify the performance of the DVR system, the following parameters are selected for experimental implementation.

1. Input filter: 1.8mH, 10A
2. Rectifier and inverter: 6 switch + diode (1200V, 50A)
3. Dc-link capacitance: 4.7mF, 900V
4. Output filter: 5mH and 40mF
5. Series transformer: 3 single-phase (220V:220V)

The controller can compensate voltage sags effectively as shown in Figure 15. Figure 15 shows the three-phase voltages for the system.

6. PWM TECHNIQUES

Space vector modulation (SVM) is nowadays the PWM technique most used to control inverters. SVM is based on the concept of approximating a rotating reference voltage space vector with those realizable on a three-phase inverter.

An optimal pulse-width-modulation is obtained on a voltage second average basis if only four switching states adjacent to the reference vector are used (SVPWM). In this case each phase is switched in sequence by switching only one inverter leg at each transition from one state to the next one. One possibility to reduce the number of switching is to use the two-phase modulation in which only two phases are modulated while the third phase is clamped to the positive (DPWMMAX) or negative (DPWMMIN) dc rail [11]. Since clamping implies in no switching losses, this technique reduces losses in each modulation interval.

SVM techniques can also be implemented by using digital scalar PWM. In this approach, non-sinusoidal modulating waveforms are introduced in a simple way. In digital scalar PWM the split and distribution of the zero space vectors duration $V_0(t_{01})$ and $V_7(t_{02})$, inside the sampling interval, can be represented by the apportioning factor $\mu = t_{01} / (t_{01} + t_{02})$ [12]. When $0 < \mu < 1$ the modulation is known as continuous modulation. The case μ=0.5 is equivalent to SVPWM. When $\mu = 0$ (DPWMMAX) or $\mu = 1$ (DPWMMIN) the modulation is known as discontinuous modulation.

Because of the simple implementation, the digital scalar PWM is used to control the inverters. The switching state functions in (18, 19, 34 and 35) are transformed to normalized reference phase voltages.

For digital implementation, time t_h is equivalent to the zero-sequence component of the pole voltage. By considering times t_a, t_b and t_c for the three sinusoidal reference signals, t_h can be written as [12]:

$$t_h = (1-\mu)\cdot(T_S - T_{max}) - \mu T_{min} \qquad (42)$$

in which T_S is the switching interval, T_{max} is the largest time interval among the three phases, and T_{min} is the smallest time interval among the same three phases. The T_{max} and T_{min} can only be defined after t_a, t_b and t_c are determined by:

$$t_k = \left(v_k^* + 1/2\right)\cdot T_S \qquad (43)$$

To verify the design of the proposed conversion system, simulations using different loads were realized. Inverter efficiencies have been calculated from the component models used with curve fitting techniques [13] for different load conditions.

DPWMMIN and DPWMMAX present the best efficiencies among the PWM techniques. It is expected since that only two phases are modulated at each modulation interval for those techniques. The MPPT algorithm presents very good results with at least 99% of the PV maximum output power. The total harmonic distortion (THD) of the supply's currents is kept below 5% for all situations. The sinusoidal PWM (SPWM) presents the highest THD

Based on characteristics discussed above, the criteria to be used to compare PWM techniques for the PV conversion system is the inverter efficiency since the differences among the MPPT efficiencies are very small when changing the PWM technique. Also, except the SPWM, the differences among the THD of the system currents are very small when changing PWM. Therefore for the proposed design, DPWMMIN or DPWMMAX should be used to control the switches in the converters 1 and 2 to improve efficiency.

7. COST ESTIMATION

The proposed system is composed basically of a PV generation system and a DVR system (Fig. 1). For the evaluation of cost, the main components are analyzed.

A. PV Generation System

The PV generation system is composed of a PV array, a dc link and a *dc–ac* converter. In the dc side it is installed a capacitor set.

In the configurations used in this paper, the PV array is always composed of 7 panels in series in such a way that the ideal dc link voltage is around 120V. When a PV generation system is connected to the grid, it is important to have the dc link voltage higher than a single panel (17V) to allow the good performance of the control. The grid has a phase rms voltage of 220V, which means that a transformer is used. A turn ratio of 10:1 has been used to connect the system to grid.

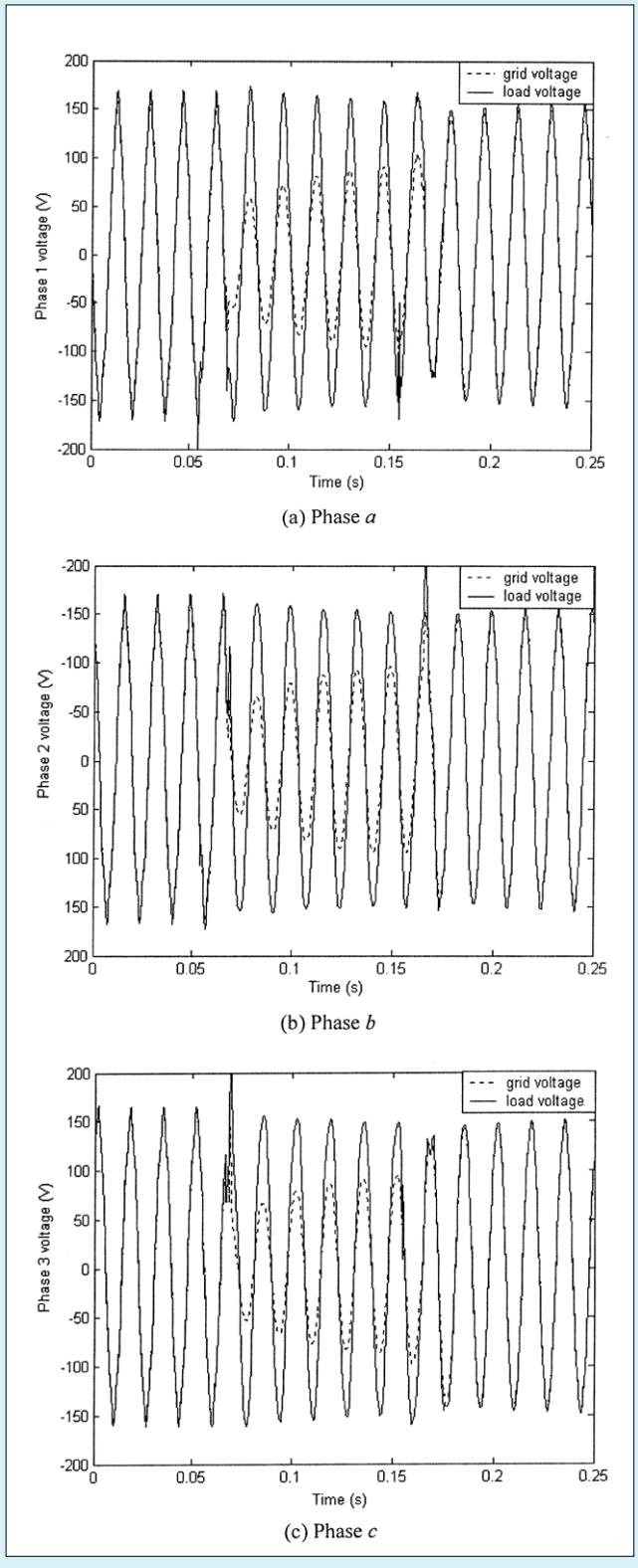

Fig. 15. Three-phase voltages during the experiment

Three possibilities of parallel connections have been tested to evaluate cost in according to generated PV power. It has been used PV arrays of 7 panels in series (700W), 14 panels (1,400W) and 28 panels (2,800W).

The dc link is composed of a capacitor of 300mF for all situations. Therefore the cost of this part of the system is kept constant. Also the cost of the dc capacitor is very low when compared to the PV array (Table 1). All prices are in US$.

Table 1. Cost of the PV System without Voltage Sag Compensation.

Components	PV array power		
	700W	1400W	2800W
PV array	3,594	7,188	14,376
Dc capacitor	22	22	22
PV converter	82	132	322
PV transformer	238	287	369

Table 2. Cost of the PV System with Voltage Sag Compensation.

Components	PV array power		
	700W	1400W	2800W
PV array	3,594	7,188	14,376
Dc capacitor	22	22	22
PV converter	132	210	396
PV transformer	271	336	450
DVR converter	82	82	82
DVR transform.	222	222	222
DVR filter	61	61	61

The PV converter is composed of six power switches with their gate drive circuits and heat sink. MOSFETs of 200V have been used. The price of transformers with turn ratio 10:1 is also considered in the total cost. The power ratings of the transformers are 600, 1,500 and 3,000VA for the PV array power of 700, 1,400 and 2,800W, respectively.

B. DVR System

The DVR system is composed of a dc-ac converter, a filter and a series transformer.

The DVR converter is composed of MOSFETs of 200V, 5A. The currents even during the voltage sag are much smaller than the currents of the PV converter.

The filter is composed of a 50μF capacitor and a 5μF inductor for all situations. The LC filter has a cut frequency of 318Hz that is approximately 5 times the grid frequency. Transformers with turn ratio 10:1 are also considered in the total cost. The power ratings of the series transformers are 600VA for all conditions since the currents have small variation when the PV array power changes (Table 2).

It is worth noting that in the proposed system there are additional components, increasing the cost of the global system. Also the PV converter and the PV transformer must have higher ratings to support the higher values of currents during the voltage sag. However, due to the high cost of the PV array when compared with the other components used in the system, the additional cost can be justified.

The critical case for the cost of the additional system occurs for the PV array of 700W. In this case, the PV system has a total cost of approximately US$ 3,936 without voltage sag compensation. With voltage sag compensation, the cost is approximately US$ 4,384 that means an additional cost of 11.4%. Increasing the PV array power, the cost of the extra components becomes less significant for the system. For the PV array of 1,400W, the additional cost is 6.5% while for the PV array of 2,800W the additional cost is only 1.1%.

8. CONCLUSION

The proposed design introduced in this paper improves functionality in grid connected photovoltaic generation systems. The design was used to do a comparative study of PWM techniques for this specific situation. The system can be connected to a three-phase system of any electric utility if a matching transformer is used. The excellent performance of the system is verified from simulated results using Matlab.

The voltage waveform in the photovoltaic array follows the reference voltage for all irradiation conditions. Besides that, the controller also compensates harmonic and reactive power. Using the design based on simulation results, it is possible to make a comparative study of different possibilities of control.

The good performance of the DVR system is verified from simulated and experimental results. The voltage waveform in the load follows the reference voltage keeping the load voltage in the rated value. Cost estimation also has been realized. It is shown that the additional components are not significant for the total cost of the system, especially if the PV array power is high.

ACKNOWLEDGMENT

The authors thank Conselho Nacional de Desenvolvimento Científico e Tecnológico (CNPq) for its financial support.

REFERENCES

1. Kuo Y.C, Liang T.J., and Chen J.F: *Novel maximum power-point-tracking controller for photovoltaic energy conversion system.* IEEE Trans. on Industrial Electronics, 2001, 48, 3, pp. 594–601.
2. Leslie L.G., Jr.: *Design and analysis of a grid connected photovoltaic generation system with active filtering function*, Master Thesis, Virginia Polytechnic Institute and State University, Blacksburg, Virginia – USA, 2003.
3. Akagi H., Kanazawa Y. and Nabae A: *Instantaneous reactive power compensator comprising switching devices without energy storage components.* IEEE Trans. on Industry Applications, 1984, 20, 3, pp. 625–630.
4. Aredes M. and Watanabe E.H.: *New control algorithms for series and shunt three-phase four-wire active power filters.* IEEE Trans. on Power Delivery, 1995, 10, 3, pp. 1649–1656.
5. Singh B., Al-Haddad K., and Chandra A.: *A review of active filters for power quality improvement.* IEEE Trans. on Industrial Electronics, 1999, 46, 5, pp. 960–971.
6. Gyugyi L., Schauder C.D., Williams S.L., Rietman T.R., Torgerson D.R. and Edris A.: *The unified power flow controller: a new approach to power transmission control.* IEEE Trans. on Power Delivery, 1995, 10, 2, pp. 1085–1093.
7. Moran S.: *A line voltage regulator/conditioner for harmonic sensitive load isolation.* IEEE Industry Applications Society Conference, 1989, pp. 947–951.
8. Mendalek N. and Al-Haddad K.: *Modeling and nonlinear control of shunt active power filter in the synchronous reference frame.* IEEE Harmonics and Quality of Power International Conference, 2000, pp. 30–35.

9. Hua C., Lin J., and Shen C.: *Implementation of a DSP-controlled photovoltaic system with peak power tracking*. IEEE Trans. on Industrial Electronics, 1998, 45, 1, pp. 99–107.
10. Chang C.S., Ho Y.S. and Loh P.C.: *Voltage quality enhancement with power electronics based devices*. IEEE Power Engineering Society Winter Meeting, 2000, 4, pp. 2937–2942.
11. Hava M., Kerkman R.J., and Lipo T.A.: *Simple analytical and graphical tools for carrier based pwm methods*. IEEE Power Electronics Specialists Conference, 1997, pp.1462–1471.
12. Jacobina B., Lima A.M.N., da Silva E.R.C., Alves R.N.C., and Seixas P.F.: *Digital scalar pulse width modulation: a simple approach to introduce non-sinusoidal modulating waveforms*. European Conference on Power Electronics and Applications, 1997, pp. 100–105.
13. Cavalcanti M.C., da Silva E.R.C., Boroyevich D., Dong W., and Jacobina C.B.: *Comparative evaluation of losses in soft and hard-switched inverters*. IEEE Industry Applications Society Conference, 2003, pp. 1912–1917.

Marcelo Cabral Cavalcanti
was born in Recife, Brazil, in 1972. He received the B.S. degree in electrical engineering in 1997 from the Federal University of Pernambuco, Recife, Brazil, and the M.S. and Ph.D. degrees in electrical engineering from the Federal University of Campina Grande, Campina Grande, Brazil, in 1999 and 2003, respectively. Since 2003, he has been at the Electrical Engineering and Power Systems Department, Federal University of Pernambuco, where he is currently a Professor of Electrical Engineering. His research interests are power electronics, renewable energy systems and power quality.

Gustavo Medeiros de Souza Azevedo
was born in Belo Jardim, Brazil, in 1981. He received the B.S. degree in electrical engineering in 2006 from the Federal University of Pernambuco, Recife, Brazil, where he is currently working toward the M.S. degree. His research interests are power electronics and renewable energy systems.

Bruno Aguiar Amaral
was born in Recife, Brazil, in 1981. He received the B. S. degree in electrical engineering in 2005 from the Federal University of Pernambuco, Recife, Brazil. His research interests are power electronics and renewable energy systems.

Francisco de Assis dos Santos Neves
was born in Campina Grande, Brazil, in 1963. He received the B.S. and M.S. degrees in electrical engineering from the Federal University of Pernambuco, Recife, Brazil, in 1984 and 1992, respectively and the Ph.D. degree in electrical engineering in 1999 from the Federal University of Minas Gerais, Belo Horizonte, Brazil. Since 1993, he has been at the Electrical Engineering and Power Systems Department, Federal University of Pernambuco, where he is currently a Professor of Electrical Engineering. His research interests are power electronics, renewable energy systems and power quality.